Available online at www.sciencedirect.com

ScienceDirect

Ceramics International 34 (2008) 1527–1532

CERAMICS
INTERNATIONAL

www.elsevier.com/locate/ceramint

Study of the bioactivity of fluorophlogopite–whitlockite ceramics

E.M. El-Meliegy *, G.T. El-Bassyouni

Department of Biomaterials, National Research Center, 12622 El-Behoos Street, Dokki, Cairo, Egypt

Received 26 February 2007; received in revised form 18 March 2007; accepted 24 April 2007
Available online 7 June 2007

Abstract

Fluorophlogopite–whitlockite phase compositions containing ceramics were prepared using Egyptian raw materials. The in vitro studies confirmed the bioactivity of the prepared mixtures. Finely divided HA layer was formed on the surface of the ceramic samples after immersion in SBF. The morphology of finely divided HA grains was found to be needle-like crystalline aggregates. The contents of calcium cations measured in SBF increased on the seventh day, compared with the first day of immersion which is attributed to dissolution. The values of phosphorous cations were slightly reduced on the seventh day, compared with the first day of immersion that is attributed to the successive dissolution and precipitation.

Keywords: Fluorophlogopite; Whitlockite; Bioactivity; In vitro

1. Introduction

The glass-ceramics based on the magnesium-aluminum silicate (MAS) system is an important class of advanced material with a wide range of applications. Mica glass-ceramics, in particular the fluorophlogopite system, are of technical interest due to their good machinability and reliable mechanical properties [1,2]. Naturally occurring micas have hydroxyl group in their structure, whereas synthetic micas involve fluorine substituting the hydroxyl group partially or completely in the structure. The effect of morphology and crystallinity of synthetic micas on the machinability of the glass-ceramics is also previously investigated [3,4].

The effect of the fluorine content and its source on the crystallization sequence of mica glass-ceramics was studied [5]. They identified the predominant crystalline phases developed during fluorophlogopite crystallization as fluorite, norbergite or fluorophlogopite depending on fluorine concentration and heat treatment regime. The crystallization of glasses in the system SiO_2–Al_2O_3–MgO–K_2O–Na_2O–F_2 results in the growth of fluorophlogopite with controlled morphology.

Although the preparation of such technologically important materials is extensively studied, their bioactivity characteristics are still indistinct and needs further study. The current paper discusses the preparation and bioactivity of porcelains containing synthetic fluorophlogopite and Mg-rich whitlockite phases. Two mixes will be prepared with different ratios of calcium phosphate and fluorophlogopite in addition to the base porcelain. In vitro study will be done by soaking the samples in SBF solution for 1 and 7 days. SEM and IR will be used to verify the compositions ability to form a surface bone-like apatite layer and evaluate the bioactivity.

2. Experimental procedure

Egyptian pure talc and feldspar raw materials were used to prepare fluorophlogopite mica porcelain. The fluorophlogopite starting glass frit composition (F) was mixed together with dicalcium phosphate (DCP) in different ratios. Two mixes (F_1 and F_2) were prepared through the addition of 50% and 75% dicalcium phosphate to the starting fluorophlogopite glass frit, respectively. The mixes were thoroughly milled and mixed in a porcelain mill for 2 h to pass 75 μm sieve. The starting compositions of the different mixes are shown in Table 1.

The thermal analysis of the milled powders was performed via Setaram instrumentation; model Labsys TG-DSC 16 in argon atmosphere and Al_2O_3 crucible up to 1150 °C.

Disc samples were prepared by pressing at 200 Mpa. The pressed discs were calcined at 950°/1 h in an electric furnace at a rate of 5 °C/min. The developed crystalline phases were

---

* Corresponding author.
E-mail address: emad.mostafa@sheffield.ac.uk (E.M. El-Meliegy).

0272-8842/$34.00
doi:10.1016/j.ceramint.2007.04.020

Table 1
Chemical composition of the different mixes

Oxides	SiO_2	Al_2O_3	MgO	K_2O	MgF_2	Na_2O	CaO	B_2O_3	P_2O_5	LOI
F	52.17	11.66	6.23	7.23	10.00	1.05	1.66	10.00	0.00	0.00
F_1	26.09	5.83	3.12	3.62	5.00	0.53	17.11	5.00	20.64	13.08
F_2	13.04	2.92	1.56	1.81	2.50	0.26	24.84	2.50	30.96	19.62

identified using XRD analysis. Samples were first ground into fine powders in an agate mortar and then scanned using Brucker D8 Advance apparatus with Cu Kα and Ni filter in the range between $2\theta = 4°$ and 70°.

The bioactivity of the prepared samples was examined by in vitro procedures [6]. SBF (electrolyte solution) was prepared by dissolving reagent grade chemicals in distilled water with the following order: NaCl, $NaHCO_3$, KCl, K_2HPO_4, $MgCl_2{\cdot}6H_2O$, 40 ml In-HCl, $CaCl_2$, Na_2SO_4 and Tris-buffer solution (Sigma Co.) while stirring.

After complete dissolution of the inorganic salts, pH was adjusted to 7.4 at room temperature. The weight of samples to SBF volume was kept constant. Samples were mounted vertically in SBF solution for two immersion periods: 1 and 7 days. At the end of each soaking period, samples were taken out of the solution and immersed for 5 min in 10 m1 of ion exchanged distilled water to stop the reaction. Specimens were then dried using ethanol at room temperature and their surfaces were analyzed using FTIR reflection spectroscopy.

FTIR analysis was used to detect the formation of hydroxyapatite on the surfaces of the specimens soaked in SBF. The reflection angle was set at 75° using FTIR reflection spectroscopy (Nicolet model 670, MA, USA).

SEM was used to study the microstructure and the variation in morphology of the different specimens using apparatus type Philips XL 30. Samples were coated with about 5 μm gold layer prior to scanning.

3. Results and discussion

The results of DSC of F, F_1 and F_2 are shown in Fig. 1. The endothermic peaks at 200 °C in F_1 and F_2 are related to the release of adsorbed surface water in the added dicalcium phosphate. The other endothermic peaks recorded at 425 °C in F_1 and F_2 are attributed to the nucleation of whitlockite. The glass transformation temperature is detected at about 400 °C. The exothermic peaks at 520 and 525 °C are related to the movement of fluorine ions in F_1 and F_2, respectively. The exothermic peak occurring at 720 and 700 °C in F and F_2 are related to the crystallization of norbergite (Mg_2SiO_4 MgF_2). The exothermic peaks recorded at 935, 950 and 950 °C in F, F_1 and F_2, respectively are related to the crystallization of fluorophlogopite. The exothermic peaks recorded at 900, and 940 °C in F_1 and F_2, respectively are related to the crystallization of whitlockite.

The TG results of DCP, F_1 and F_2 show one step reaction. The weight loss is related to the proportion of dicalcium phosphate (DCP). The weight loss % is found 9.6, 15 and 19.5 in F_1, F_2 and DCP, respectively.

The phase analysis of the fluorophlogopite glass-ceramic (F) was previously discussed [7]. Fluorophlogopite is the developed mineral phase together with appreciable amount of forsterite as secondary mineral phase. The formation of forsterite phase is controlled by the ratio of $MgO + MgF_2/SiO_2$ during a subsequent prolonged exposure to heat treatment [8,9]. Forsterite is no longer being formed with achieving the optimum ratio of $MgO + MgF_2/SiO_2$.

The XRD patterns for F_1 and F_2 mixes in addition to the XRD of dicalcium phosphate fired at 950 °C are shown in Fig. 2. The mix F_1 shows the development of fluorophlogopite KMg_3 $(AlSi_3O_{10})F_2$ and magnesium rich whitlockite $(Ca,Mg)_3(PO_4)_2$ phases. With increasing the content of

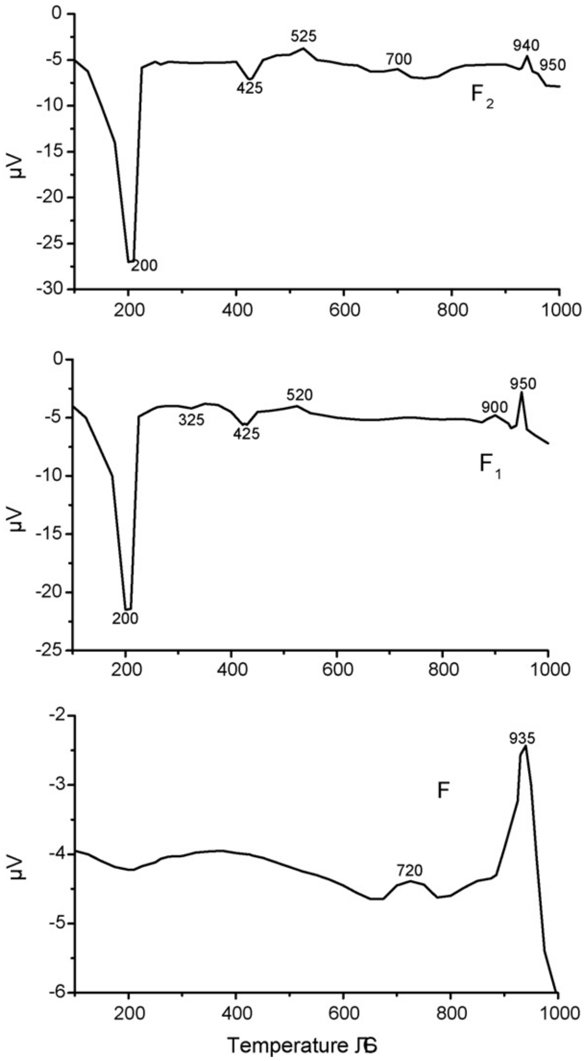

Fig. 1. DSC of the powders of different studied mixes.

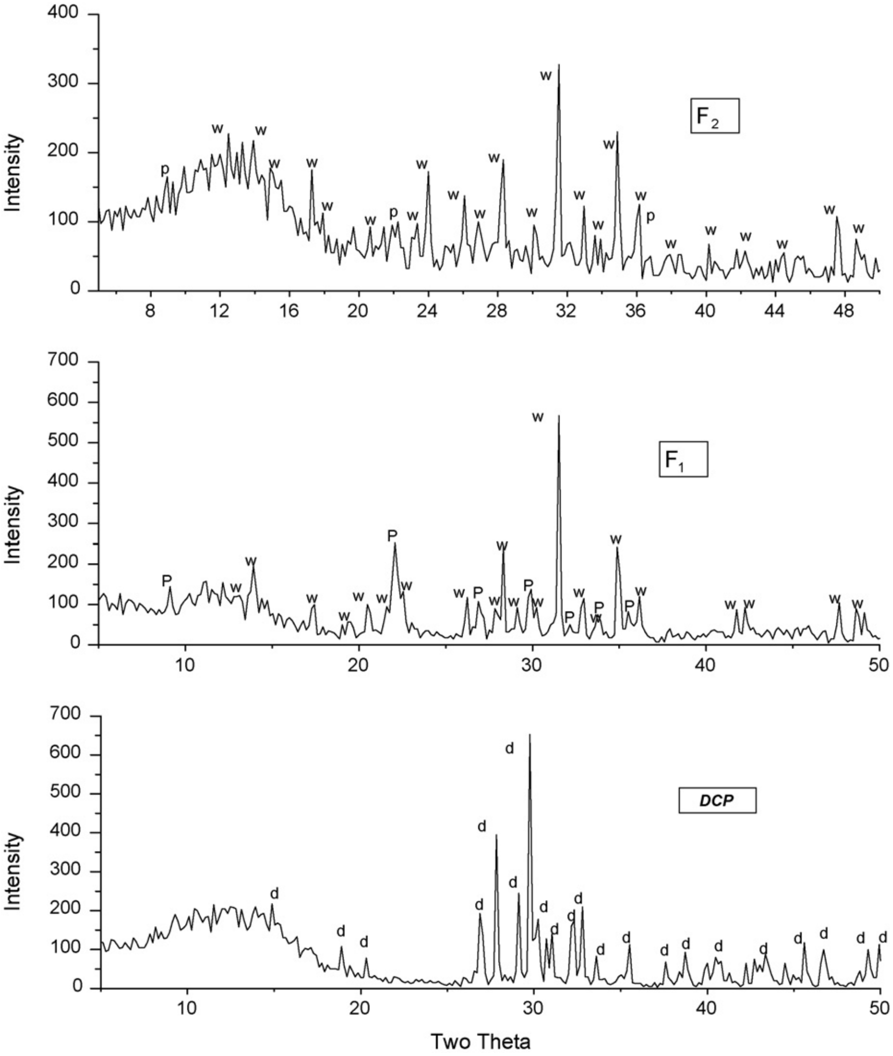

Fig. 2. XRD of different mixes fired at 950 °C/1 h. D: dicalcium phosphate; F: fluorophlogopite; W: whitlockite.

dicalcium phosphate in mix F_2, the whitlockite increases and the fluorophlogopite content decreases.

Bioactive ceramics are capable of initiating HA formation during soaking in SBF. The formation of HA on the surface of the implant is considered the key factor for creation of bone-bonding and potential bone-forming ability [10,11]. In the present work, in vitro studies were performed for the F, F_1 and F_2 samples.

The levels of calcium and inorganic phosphorus in SBF were measured sequentially after the withdrawal of soaked samples. The values of Ca^{2+} ions are found to increase in the case of all samples (F, F_1 and F_2) in the seventh day compared with their corresponding values in the first day of immersion. The results indicate the dissolution (degradation) of Ca^{2+} ions from the immersed samples. On the other hand, the values of phosphorous ions in the seventh day of immersion are slightly reduced compared with the first day of immersion. The results indicate the successive deposition and precipitation of P-ions on the surface of the soaked samples. The results are agreed by those previously recorded [10,11]. The formation of an amorphous calcium phosphate layer is favored on the top of the soaked samples in the first day, while subsequent crystallization to carbonated HA (C-HA) was favored in the seventh day of immersion. The dissolution rates in vitro are found directly proportional to the content of calcium phosphate as previously recorded [12].

The surface changes analyzed using FTIR reflection spectra are shown in Fig. 3. In case of F sample immersed for 1 day, the peak at 450 cm^{-1} is ascribed to the Si–O–Si bending vibration, while the peak at 926 cm^{-1} is attributed to Si–OH stretching vibration [13]. The peaks located at 500–600 cm^{-1} are assigned as P–O bending vibration mode in the $[PO_4]$ tetrahedral [14]. Ca–P amorphous layer was formed on the surface of the immersed F sample [15]. The spectra showed band at 1277 cm^{-1}, which is usually assigned to P–O bonds [16]. After increasing the soaking time up to 1 week, gradual reduction in splitting of the major PO_4 bands and their corresponding intensities was observed. The result suggests the formation of poorly crystallized Ca-phases [16].

The FTIR spectrum of F_1 immersed for 1 day showed the accumulation of dicalcium phosphate into the structure. A strong band assigned for asymmetric stretching mode of PO_4^{3-} is recorded at 1260 cm^{-1}, together with bands at 1048 and

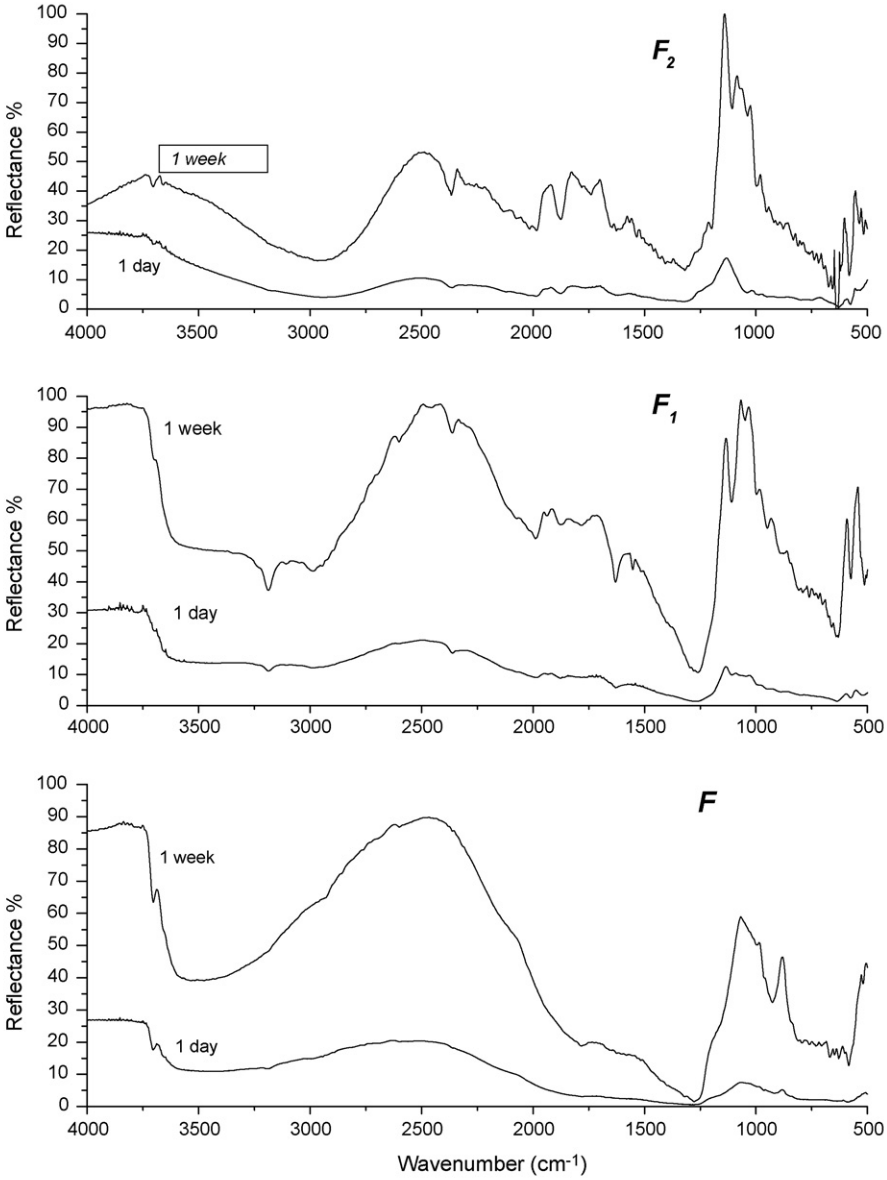

Fig. 3. IR spectra of different samples soaked in SBF.

$1109\ cm^{-1}$. Bands recorded in the range of $407–455\ cm^{-1}$ are assigned for the bending mode of $PO_4{}^{3-}$ [17].

The bands assigned for both stretching and bending mode of $(PO_4)^{3-}$ vibration confirm the presence of Ca-phosphate structure. The splitting of bands in the range of $500–600\ cm^{-1}$ is assigned for $(PO_4)^{3-}$ bending mode. The peak at $631\ cm^{-1}$ is ascribed to OH^- band that clearly characterize the HA formation in sample F_1. After 1 week of immersion, F_1 shows a gradual reduction in the splitting and intensities of the $(PO_4)^{3-}$ bands, which confirms coating with a thin layer of calcium phosphate.

In case of F_2 samples, all the characteristic bands of Ca–P mentioned before are clearly detected in the first day of immersion. As the immersion time increase, fine splitting of P–O bending bands indicates formation of a finely crystallized HA in the seventh day of immersion. The finely crystallized HA layer was created favorably by heterogeneous precipitation from the solution, when it became supersaturated [18,19]. This finely divided layer disappears in F sample, while the above-mentioned amorphous layer was formed instead [20].

The results of SEM for samples F_1 and F_2 soaked for different times are shown in Figs. 4–7. In case of F_1 immersed for 7 days, SEM photographs show a coating layer on the surface of the sample. The SEM of the F_2 specimen portrays a thick layer overlapping the substrate surface which becomes more clear and detailed at higher magnification.

The formation of finely divided HA layer in both F_1 and F_2 soaked for different times was realized. The coating is homogeneously covering the surface of the samples. The morphology of HA particles is found to be uniform in shape and size. The morphology of the HA layer is verified into separated particles that coalesce together in case of F_2, while the particles are slightly verified in case of F_1. This may be due to the differential grain growth of deposited HA grains with different

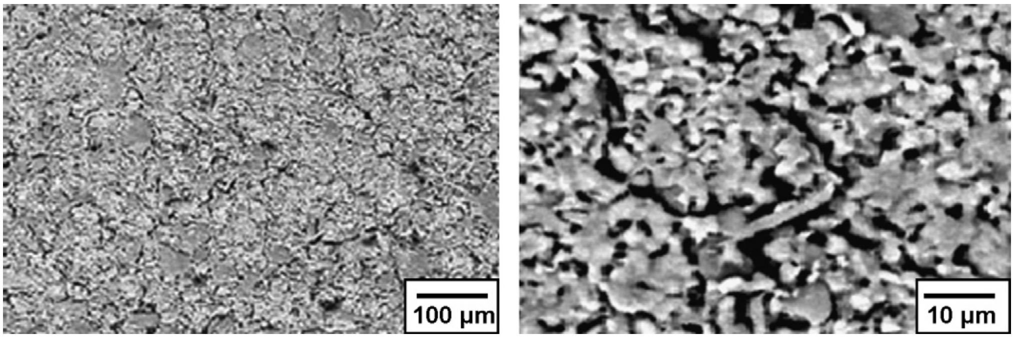

Fig. 4. SEM of F_1 soaked for 1 day in SBF.

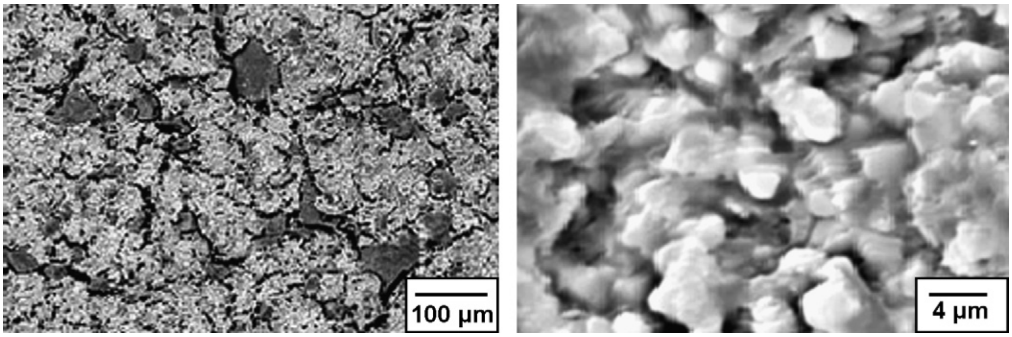

Fig. 5. SEM of F_2 soaked for 1 day in SBF.

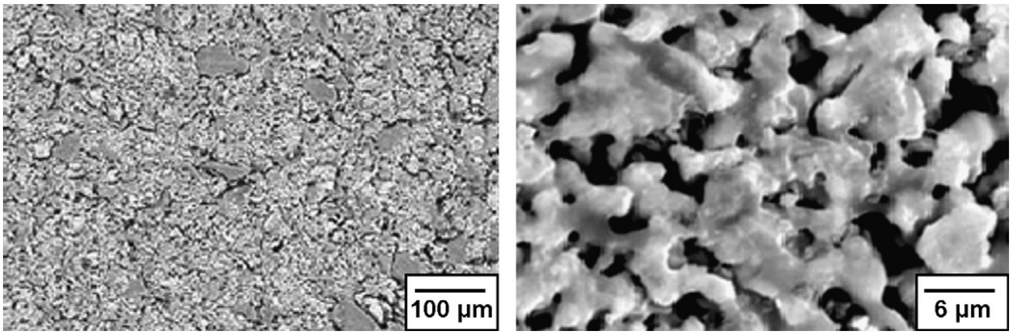

Fig. 6. SEM of F_1 soaked for 1 week in SBF.

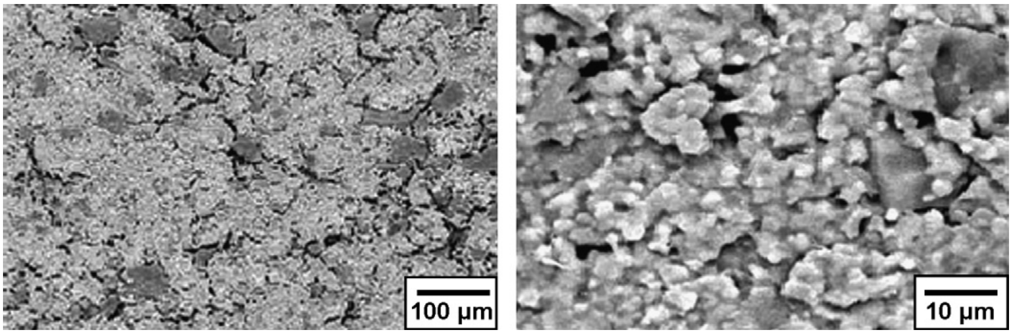

Fig. 7. SEM of F_2 soaked for 1 week in SBF.

compositions. At higher magnification, the spherical particles are made of numerous crystalline aggregates. The surface morphology changes upon immersion and a layer of spherical particles fully integrates into the structure causing aggregation and difficulty of separation.

4. Conclusion

The fluorophlogopite is the sole crystalline phase of the base glass-ceramic (F). After the addition of calcium phosphate in F_1 and F_2, Mg-rich whitlockite became predominant phase together with fluorophlogopite phase. In vitro studies indicates the formation of HA on the surface as a key factor for the creation of bone-bonding and bone-forming ability. Finely divided HA layer was formed in both F_1 and F_2 soaked for different times. The morphology is found to be of uniform spherical particles. The spherical particles are made of numerous crystalline aggregates. The bands assigned for both stretching and bending mode of vibration of $(PO_4)^{3-}$ in IR patterns confirm the presence of HA structure. The values of Ca^{2+}ions increases on the seventh day compared with first day of immersion due to dissolution. The values of phosphorous ions are slightly reduced on the seventh day compared with the first day of immersion due to the successive dissolution and precipitation.

References

[1] C.K. Chyung, G.H. Beall, D.G. Grossman, Electron microscopy and structure of materials, in: Proceedings of the Fifth International Materials Symposium, University of California Press, Beerkeley, CA, 1971 p. 1167.

[2] M. Goswami, A. Sarkar, T. Mirza, V.K. Shrikhande, K.R. Gurumurthy, G.P. Kothiyal, Study of some thermal and mechanical properties of magnesium aluminum silicate glass ceramic, Ceram. Int. 28 (2002) 585–592.

[3] D. Baik, K.S. No, J.S. Chun, Y.Y. Yoon, H.Y. Cho, A comparative evaluation method of machinability of mica based glass ceramics, J. Mater. Sci. 30 (1995) 1801–1806.

[4] D.S. Baik, K.S. No, J.S. Chun, H.Y. Cho, Effect of the aspect ratio of mica crystals and crystallinity on micro hardness and machinability of mica glass ceramics, J. Mater. Process. 67 (1997) 50–54.

[5] L.J. Radonjic, L.J. Nikolic, The effect of fluorine and concentration on the crystallization of machinable glass-ceramics, J. Eur. Ceram. Soc. 7 (1991) 11–16.

[6] P. Sepulveda, J.R. Jones, L.L. Hench, In vitro dissolution of melt-derived and sol–gel derived 58S bioactive glasses, J. Biomed. Mater. Res. 61 (2002) 301–311.

[7] E.M. El-Meliegy, Machinable spodumene-fluorophlogopite glass ceramic, Ceram. Int. 30 (2004) 1059–1065.

[8] E.A. Mustafa, Fluorophlogopite porcelain based on talc–feldspar mixture, Ceram. Int. 27 (2001) 9–14.

[9] E.M. El-Meliegy, E. Hamzawy, Celsian-fluorophlogopite porcelain based on Egyptian talc, Adv. Appl. Ceram. 104 (2) (2005) 92–96.

[10] L.L. Hench, Bioactive ceramics, in bioceramics, in: P. Ducheyne, J.E. Lemonis (Eds.), Material Characteristics Versus In Vivo Behavior, The New York Academy of Sciences, New York, 1988, pp. 54–71.

[11] P. Ducheyne, S. Radin, L. king, The effect of calcium phosphate ceramic composition and structure on in vitro behavior, I. Dissolution., J. Biomed. Mat. Res. 27 (1993) 25–34.

[12] M. Jarcho, Calcium phosphate ceramics as hard tissue prosthetics, Clin. Orthop. 157 (1981) 259–278.

[13] S. Radin, P. Duchyne, B. Rothman, A. Conti, The effect of in vitro modeling conditions on the surface reactions of bioactive glass, J. Biomed. Mat. Res. 35 (1997) 526–539.

[14] G. Orcel, J. Phalippou, L.L. Hench, Structural changes of Silica xerogels during low temperature dehydration, J. Non-Cryst. Solids 88 (1986) 114–130.

[15] R.F. Le Geros, G. Bond, R. Le Geros, Type of H_2O in human enamel and in precipitated apatite, Calcify. Tissue Res. 26 (1978) 111–118.

[16] C.Y. Kim, A.E. Clark, L.L. Hench, Early stages of calcium–phosphate layer formation in bioglasses, J. Non-Cryst. Solids 113 (1989) 195–202.

[17] M.M. Pereira, A.E. Clark, L.L. Hench, Calcium phosphate formation on Sol–gel-derived bioactive glasses in vitro, J. Biomed. Mat. Res. 28 (1994) 693–698.

[18] S. Radin, P. Ducheyne, The effect of calcium phosphate ceramic composition and structure on in vitro behavior: II. Precipitation, J. Biomed. Mat Res. 27 (1993) 35–45.

[19] J.C. Heughebaert, R.Z. Le Geros, A. Guilhem, G. Bonel, Physicochemical characterization of deposits associated with HA ceramics implanted in nonosseous sites, J. Biomed. Mater. Res. Appl. Biomat. A_3 (1988) 257–268.

[20] S. Radin, P. Ducheyne, The effects of serum proteins on solution induced surface transformations of bioactive ceramics, J. Biomed. Mater. Res. 30 (1995) 273–297.